

Near-linear response of mean monsoon strength to a broad range of radiative forcings

William R. Boos^{a,1} and Trude Storelvmo^a

^aDepartment of Geology and Geophysics, Yale University, New Haven, CT 06520

Edited by Robert E. Dickinson, The University of Texas at Austin, Austin, TX, and approved December 9, 2015 (received for review August 27, 2015)

Theoretical models have been used to argue that seasonal mean monsoons will shift abruptly and discontinuously from wet to dry stable states as their radiative forcings pass a critical threshold, sometimes referred to as a “tipping point.” Further support for a strongly nonlinear response of monsoons to radiative forcings is found in the seasonal onset of the South Asian summer monsoon, which is abrupt compared with the annual cycle of insolation. Here it is shown that the seasonal mean strength of monsoons instead exhibits a nearly linear dependence on a wide range of radiative forcings. First, a previous theory that predicted a discontinuous, threshold response is shown to omit a dominant stabilizing term in the equations of motion; a corrected theory predicts a continuous and nearly linear response of seasonal mean monsoon strength to forcings. A comprehensive global climate model is then used to show that the seasonal mean South Asian monsoon exhibits a near-linear dependence on a wide range of isolated greenhouse gas, aerosol, and surface albedo forcings. This model reproduces the observed abrupt seasonal onset of the South Asian monsoon but produces a near-linear response of the mean monsoon by changing the duration of the summer circulation and the latitude of that circulation’s ascent branch. Thus, neither a physically correct theoretical model nor a comprehensive climate model support the idea that seasonal mean monsoons will undergo abrupt, nonlinear shifts in response to changes in greenhouse gas concentrations, aerosol emissions, or land surface albedo.

monsoons | tropical climate | tipping points

Monsoons deliver water to billions of people, so catastrophe would likely result if a gradual and small change in a forcing produced a comparatively abrupt and large change in monsoon strength. Previous studies (1, 2) used theoretical models to argue that monsoons will undergo exactly this sort of abrupt transition if anthropogenic or natural forcings exceed a critical threshold, which they referred to as a “tipping point” (3). Changes in land use or atmospheric aerosols sufficient to increase local top-of-atmosphere albedo to 0.5 have been predicted to cause a shift in the Indian summer monsoon from its current wet state to a dry state (1). The idea that anthropogenic climate forcings might produce an abrupt shutdown of some monsoons has become prominent (3, 4), even though some argue that this is unlikely to occur in the next century (5).

Paleoclimate records contain abundant evidence for abrupt changes in various measures of monsoon strength (6, 7). However, such records typically measure variations at a particular location and so may not distinguish between a nonlinear response of the entire monsoon and a more gradual, linear shift of a spatial pattern with sharp horizontal gradients. It is also unclear whether mechanisms that govern monsoon changes on orbital to geological time scales are relevant for the response to anthropogenic forcings. However, even if proxy records of past monsoons are ambiguous, the modern seasonal cycle contains evidence for the abrupt response of monsoons to a radiative forcing: South Asian summer monsoon onset occurs more rapidly than can be explained by a linear response to the annual cycle of insolation (8, 9). Although the cause of this nonlinear seasonal evolution is the subject of active research (10, 11), it seems plausible that the same mechanism might produce an abrupt response of the seasonal mean monsoon to an imposed seasonal mean forcing.

These results motivate our examination of how monsoon strength scales with a range of forcings. In particular, we use a simple energetic theory and an ensemble of global climate model (GCM) integrations to determine whether the summer mean strength of tropical monsoons will change discontinuously in response to a large range of radiative forcings.

Analytical Results

A simple model of a monsoon is obtained by assuming thermally direct flow from an ocean toward a tropical continent,

$$v = \frac{\kappa}{\epsilon_1} \frac{\partial T}{\partial y} \quad [1]$$

where the wind v is positive for low-level flow from ocean to land, T is tropospheric temperature, κ is the ratio of the gas constant to the specific heat of air, and ϵ_1 is a frictional damping constant. Steady-state conservation equations for T and humidity q , which represent anomalies relative to a tropical mean background state, are used to couple v to the energy sources provided by surface sensible heat flux H , surface evaporation E , and the atmospheric radiative flux convergence R ,

$$a_{TV} \frac{\partial T}{\partial y} - M_s \frac{\partial v}{\partial y} = P + R + H \quad [2]$$

$$a_q v \frac{\partial q}{\partial y} + M_q \frac{\partial v}{\partial y} = -P + E. \quad [3]$$

Here M_s is the dry thermal stratification and the term $M_s \partial_y v$ in Eq. 2 represents adiabatic cooling in the circulation’s rising

Significance

Previous studies have argued that monsoons, which are continental-scale atmospheric circulations that deliver water to billions of people, will abruptly shut down when aerosol emissions, land use change, or greenhouse gas concentrations reach a critical threshold. Here it is shown that the theory used to predict such “tipping points” omits a dominant term in the equations of motion, and that both a corrected theory and an ensemble of global climate model simulations exhibit no abrupt shift in monsoon strength in response to large changes in various forcings. Therefore, although monsoons are expected to change in response to anthropogenic forcings, there is no reason to expect an abrupt shift into a dry regime in the next century or two.

Author contributions: W.R.B. designed research, produced analytical results, and performed and analyzed GCM runs; W.R.B. and T.S. wrote the paper; T.S. designed GCM aerosol emissions and interpreted aerosol response.

The authors declare no conflict of interest.

This article is a PNAS Direct Submission.

Data deposition: Global climate model output used in this study is available from the authors.

¹To whom correspondence should be addressed. Email: billboos@alum.mit.edu.

This article contains supporting information online at www.pnas.org/lookup/suppl/doi:10.1073/pnas.1517143113/-DCSupplemental.

branch (where low-level air converges). This system represents the state of the full depth of the troposphere, with T the temperature anomaly of the entire tropospheric column and with winds changing sign in the midtroposphere (i.e., upper-tropospheric flow is given by $-\nu$). Both T and q have units of energy, having absorbed constants for the specific heat and latent heat of vaporization, respectively. The moisture stratification M_q appears in the term representing low-level moisture convergence ($M_q \partial_y \nu$), which, in the tropics, is the leading term that balances removal of water by precipitation P . The constants a_T and a_q express the efficiency with which horizontal advection alters T and q , respectively. A common, simple closure for precipitation has P increase with column moisture and decrease as rising free-tropospheric temperatures make the column more stable to moist convection,

$$P = \frac{q - T}{\tau_c^*} \mathcal{H}(q - T). \quad [4]$$

Here τ_c^* is the time scale over which moist convection relaxes the troposphere toward a moist adiabatic state in which $q = T$; when $T > q$, the column is sufficiently warm and dry so as to be stable to moist convection. The Heaviside function \mathcal{H} ensures nonnegative precipitation. This system is identical to the nonrotating equations for the first baroclinic mode of the tropical troposphere used in the Quasi-Equilibrium Tropical Circulation Model (QTCM), which numerous studies have used to advance understanding of monsoons (12, 13). We neglect rotation, for consistency with previous theoretical models used to argue for the existence of monsoon tipping points (2).

We combine Eqs. 1–4 into a cubic polynomial in ν and solve it analytically using a standard set of parameter values (12). The solution (see *Materials and Methods* and *SI Appendix* for methodological details) shows that when a net source of energy is supplied to the atmosphere over the monsoonal continent so that $Q = E + H + R > 0$, low-level winds blow from ocean to land, where precipitating ascent occurs ($\nu > 0$ and $P > 0$, Fig. 1A). The circulation exports energy from its ascending branch to balance the imposed energy source Q ; the low-level import of moisture is more

than compensated for, in the vertically integrated energy budget, by the export of dry static energy by upper-tropospheric divergent flow. This compensation is captured by the fact that the gross moist stability, $M_s - M_q$, is positive but much less than the dry stability, M_s , consistent with studies of the energetics of large-scale tropical flow (14, 15). When $Q < 0$, the circulation reverses ($\nu < 0$) and precipitation is suppressed in the continental subsiding flow ($P = 0$), typical of winter conditions in monsoon regions.

As Q becomes positive, precipitation smoothly increases from zero. There are no discontinuities in P or ν as Q is varied, and their response to Q is only slightly nonlinear for $Q > 0$. The sensitivities of ν and P to Q change as Q passes through zero, because, in subsiding regions, the diabatic heat source of precipitation does not offset adiabatic heating due to vertical motion (i.e., precipitation is nonnegative). There is no critical value of Q at which P and ν change discontinuously, and thus no threshold or tipping point at which the monsoon could be argued to abruptly shut down.

In their model of monsoon tipping points, Levermann et al. (2) set M_s in Eq. 2 to zero, thereby neglecting the adiabatic cooling of ascending air. The transport of moisture from ocean to land then provides an energy source that effectively makes the gross moist stability negative, and the circulation imports energy into the ascending column to balance the net divergence of radiative energy. Levermann et al. (2) and related studies (1, 4) stated that this import of moisture provides a “moisture advection feedback” that causes abrupt shifts of monsoons between wet and dry states. They also notably omitted the term $M_q \partial_y \nu$ in Eq. 3, which represents horizontal convergence of moisture. Moisture convergence and adiabatic cooling are widely acknowledged to be leading terms in the moisture and thermodynamic equations, respectively, by many theoretical and observational studies over the past 50 y (14, 16–19); these two terms do not simply cancel, and neglecting them in any model of a monsoon is not a matter of theoretical preference but a fundamental error.

We modify our analytical model to demonstrate that the moisture advection feedback and the threshold behavior it permits are artifacts of neglecting the static stability. We set $M_s = 0$ and change

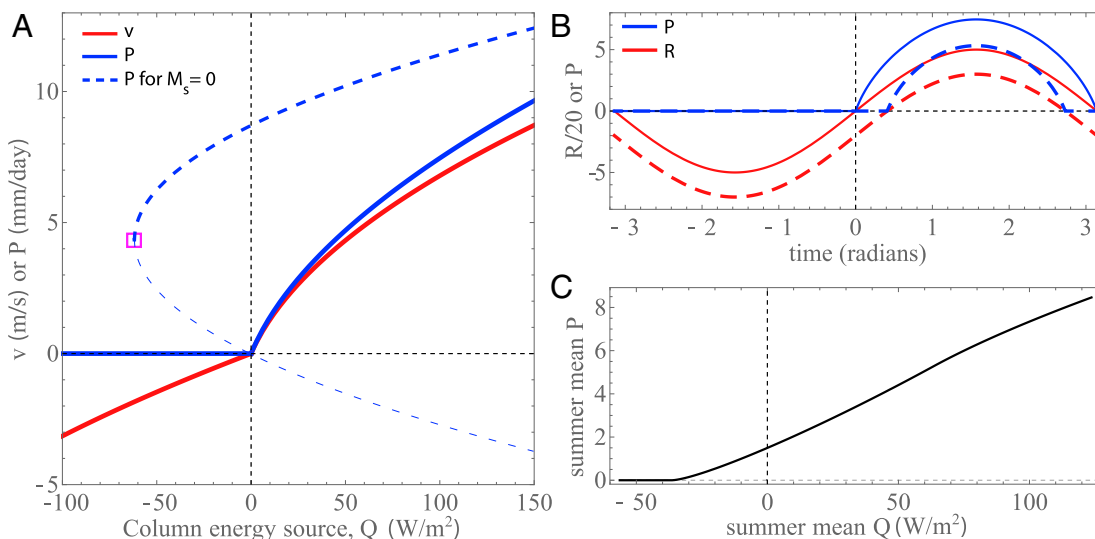


Fig. 1. Response of analytical model of a monsoon to forcing variations. (A) Low-level landward wind (red, meters per second) and land precipitation (solid blue, millimeters per day) as a function of the vertically integrated atmospheric energy source Q for our standard analytical model. Thick dashed line shows precipitation when the static stability is artificially set to zero, with the magenta square marking the critical value of Q below which no solution exists and the thin dashed blue line when the nonphysical solution. (B) Annual cycle of radiative forcing (red) and precipitation (blue) when the standard model is used to represent the daily mean response to daily mean Q . Solid lines are for a sinusoidal forcing with amplitude $100 \text{ W}\cdot\text{m}^{-2}$ and zero mean, and dashed lines are for the same forcing with a $-40 \text{ W}\cdot\text{m}^{-2}$ offset. Time is in radians with spring equinox at zero. (C) Precipitation as a function of Q with both averaged over the half of the year centered on the peak Q and the offset in Q varied from $-120 \text{ W}\cdot\text{m}^{-2}$ to $60 \text{ W}\cdot\text{m}^{-2}$.

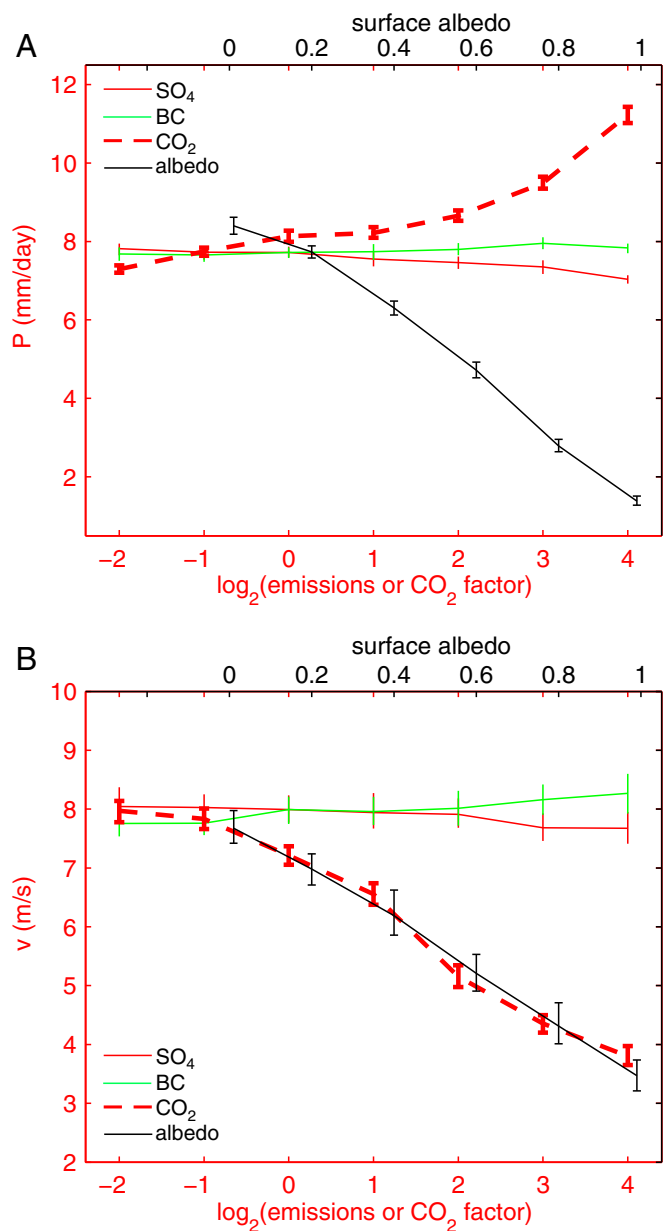


Fig. 2. Response of monsoon (A) precipitation and (B) circulation (i.e., meridional wind) to an ensemble of forcings in the GCM. Black line is for albedo forcings, with India’s surface albedo noted on the top abscissa. Dashed line is for CO₂ forcings, and thin red and green lines are for sulfate and BC emission forcings, with the scaling factor for CO₂ concentrations or aerosol emissions shown on the bottom abscissa. Vertical bars show the 95% confidence interval for the mean, estimated by 2,000 iterations of a bootstrap. Precipitation was averaged from May through September over the blue box shown in Fig. 3A, and the circulation is a slightly modified form of an existing “southerly shear” index (21) obtained by averaging the meridional wind difference between 850 hPa and 200 hPa over regions of strong low-level northward monsoon flow: (85°E–100°E, 15°N–30°N) and (30°E–55°E, 15°S–0°N).

the sign of a_T so that the associated advection represents temperature advection due only to lower tropospheric winds, consistent with Levermann et al. (2). The latter change is minor, however, and the key change is setting $M_s = 0$ (see discussion in *SI Appendix*). With these two modified parameters, precipitating monsoonal ascent occurs for all $Q > -61.3 \text{ W}\cdot\text{m}^{-2}$ (dashed blue curve in Fig. 1A). The precipitating monsoon circulation would abruptly cease (i.e., no solutions exist) if atmospheric aerosols, land

use change, or some other forcing caused Q to become more negative than this critical threshold. However, this only occurs when the static stability is erroneously assumed to be zero and the monsoon circulation thus becomes energetically indirect, converging energy into its ascending branch. Observational estimates of the energy budget are consistent with our assertion that $Q > 0$ in summer monsoon regions and that monsoons export energy from their ascending branches (20).

Global Climate Model Results

Although Eqs. 1–4 are a more complete model than that used in previous studies arguing for the existence of tipping points, this system neglects planetary rotation, nonlinear momentum advection, and the wind dependence of ocean surface evaporation, each of which has been argued to cause the abrupt seasonal onset of the South Asian monsoon (9, 10). Instead of adding representations of these processes to our theoretical model, we integrate the coupled ocean–atmosphere Community Earth System Model (CESM), at a nominal 1° horizontal resolution, to determine whether seasonal mean monsoon strength exhibits a threshold response to large variations in four types of forcings (see *Materials and Methods* for details). In particular, we vary greenhouse gas concentrations, anthropogenic sulfate aerosol emissions, and anthropogenic black carbon (BC) aerosol emissions independently from 0.25 to 16 times present-day values in three series of integrations. In a fourth set of integrations, we vary the land surface albedo of continental India from zero to unity (see summary in *SI Appendix, Table S2*).

The summer mean strength of the South Asian monsoon exhibits no discontinuous or abrupt response to variations in any of these forcings. As the surface albedo of continental India is increased from zero to unity, South Asian monsoon precipitation and circulation strength both decrease near linearly as a function of albedo [Fig. 2; the meridional wind average used to define the circulation strength is based on an existing monsoon index (21) and is a good analog for v in the analytical model]. Increased albedo weakens precipitating ascent and low-level monsoon westerlies (Fig. 3B) because land absorbs less shortwave radiation and thus emits less enthalpy into the atmospheric column. This reduces Q in a basic state where $Q > 0$, so P decreases as in our analytical model. Although our albedo forcing is idealized and not intended to represent realistic changes in land use, this nearly linear response disproves the idea that the South Asian monsoon will abruptly switch into a dry state as its local energy source is reduced. These albedo variations span the maximum possible range and produce variations in Q larger than any that might be produced by plausible changes in land use or atmospheric aerosols; they far exceed the value of 0.5 at which monsoon shutdown was predicted to occur by previous studies (1, 3). Although we only changed the albedo of nonelevated parts of India, it has been shown that South Asian monsoon strength is more sensitive to surface heat flux perturbations in this region than in the Tibetan Plateau and Himalayas (22, 23). Additionally, even though previous studies of tipping points did not argue for hysteresis in monsoons, we note that there is no evidence for hysteresis as albedo changes in time (see *SI Appendix*).

Enhanced CO₂ concentrations cause increased precipitation over all of South Asia in this GCM, together with a weakening and northward shift of low-level westerlies (Fig. 3A). Because CO₂ is well mixed, its variations provide a more spatially uniform forcing than albedo changes. Thus, although albedo can be thought to primarily alter Q , CO₂ changes leave Q relatively unchanged and modify M_s and M_q through the temperature dependence of those variables. A horizontally uniform increase in temperature at fixed relative humidity will increase M_q following Clausius–Clapeyron; M_s also increases as the troposphere moves to a warmer moist adiabat and as deep convection reaches higher altitudes. Some studies have found that M_s , M_q , and the quantity $M_s - M_q$ all increase in GCMs as the tropics warm (24), which, for negligible

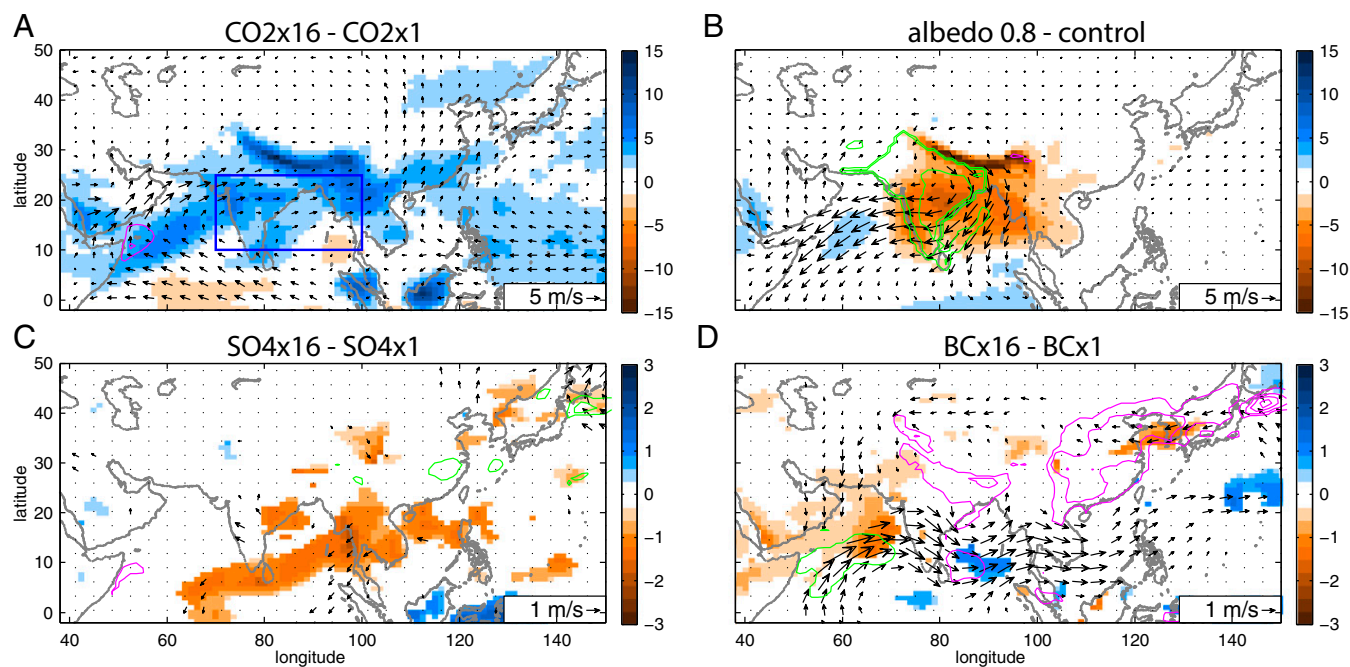


Fig. 3. GCM anomalies of precipitation (shading, millimeters per day), 850-hPa horizontal wind (vectors), and vertically integrated atmospheric energy source Q (contours, magenta positive and green negative) produced by select forcings. Plots only show precipitation and Q anomalies significant at the 5% level and wind anomalies with a zonal or meridional component significant at the 5% level, as estimated by a Student t test. Panels show differences between integrations with (A) 16 \times and 1 \times present-day CO_2 , (B) India's surface albedo of 0.8 and the default land surface albedo, (C) 16 \times and 1 \times modern sulfate emissions, and (D) 16 \times and 1 \times modern BC aerosol emissions. All quantities are averaged May–September. Contour interval for Q anomalies is 50 $\text{W}\cdot\text{m}^{-2}$ in A and B and 10 $\text{W}\cdot\text{m}^{-2}$ in C and D; note the change in color scale and reference vector between A and B and C and D.

change in Q , requires a slowing of the circulation and an increase in rainfall. This is exactly what is seen in our simulations. Although monsoon precipitation increases faster than linearly as a function of $\log_2(\text{CO}_2)$, it scales near linearly until CO_2 concentrations reach 4 \times modern values. Circulation strength scales linearly over almost the entire range of CO_2 forcings, with some evidence for a saturation of circulation strength at very low CO_2 concentrations.

The monsoon exhibits a comparatively weak response to 64-fold variations in Asian anthropogenic emissions of either BC or sulfate aerosols and their precursors (thin green and red lines in Fig. 2). The weakness of this change may seem surprising given that previous studies argued that anthropogenic aerosols have reduced South Asian rainfall (25, 26). However, our strong aerosol forcings produce radiation and precipitation changes comparable in magnitude to those of previous studies (see *SI Appendix*). The full range of our albedo and CO_2 forcings is simply much larger than any expected to arise from anthropogenic causes, whereas our aerosol changes are closer to the observed difference between preindustrial and modern periods; we plot all of these responses on the same axes only for convenience in assessing whether thresholds exist, not because of any expectation that the magnitude of the responses should be similar.

Major features of the response to aerosols can also be understood in terms of our analytical model. Enhanced burdens of BC aerosol (e.g., absorbing soot) increase Q by increasing the absorption of shortwave radiation, which strengthens the monsoon. When anthropogenic BC emissions are increased 16-fold compared with modern values, Q increases by 10–20 $\text{W}\cdot\text{m}^{-2}$ over the Indo-Gangetic plain, Bay of Bengal, and East Asia (Fig. 3D), the regions where BC burden rose most strongly (see *SI Appendix*). Low-level cyclonic flow intensifies around this region of enhanced Q . The statistically significant precipitation increase is much smaller in horizontal extent than the change in Q , consistent with the fact that there is more precipitable water over the Bay of Bengal than over East Asia; the vertical structure of BC heating may also suppress precipitation. Precipitation and Q are reduced over the Arabian Sea, and that Q

decrease comprises enhanced outgoing longwave radiation resulting from reduced high-level cloudiness, which might in turn be caused by BC stabilization of the atmospheric column. There is also reduction in Arabian Sea sea surface temperature (SST), so BC aerosols might alternatively weaken the monsoon by reducing the cross-equatorial SST gradient (25, 27), but cross-equatorial flow and low-level westerlies actually strengthen in our GCM. Sea salt aerosol also increases over the Arabian Sea, presumably because of the intensification of the Somali jet, which may also contribute to the rain and cloud response.

Increased sulfate aerosol produces changes that are of similar magnitude but more spatially uniform than those induced by BC aerosol. A 16-fold increase in sulfate emissions reduces rainfall by 1–2 $\text{mm}\cdot\text{d}^{-1}$ over large parts of the North Indian Ocean and South Asia (Fig. 3C). However, sulfate produces a change in Q (Fig. 3C) that is much weaker and less horizontally extensive than that produced by BC. Sulfate aerosol also produces only a slight weakening of monsoon winds. All of this seems to occur because sulfate acts primarily through a tropics-wide cooling and associated reduction in precipitable water, which, in our analytical model, would reduce P by reducing M_q rather than by changing Q . Like CO_2 , sulfate aerosol may thus act primarily via spatially homogeneous temperature change, whereas BC aerosol and land surface albedo act primarily to alter horizontal gradients in Q . To our knowledge, this aspect of the response to BC vs. sulfate aerosol has not been discussed and may complicate understanding of the response to realistic superpositions of sulfate and BC aerosol. For our present purpose, these are all side issues, with the main point being that no threshold response is seen in response to a large range of aerosol changes.

Response of Monsoon Duration and Location

Previous studies have argued that the mechanism responsible for the observed abrupt seasonal onset of the South Asian monsoon might produce an abrupt response to forcings that vary on geological time scales (28). In contrast, other work has shown that

Other simulations of next-century climate have produced evidence for a linear relationship between trends in regional precipitation and trends in tropical mean temperature (33). In addition, the South Asian monsoon exhibited a nearly linear response to large changes in elevated topography in other GCM simulations (23). Thus, outside of a theory that omitted a dominant term in the equations of motion, we know of no evidence supporting the idea that monsoons will shut down in response to anthropogenic forcings. Monsoons may have a strong response to anthropogenic forcings, but current theory and numerical models indicate that this response will be nearly linear.

Materials and Methods

A full derivation of the analytical model is provided in the description of the QTCM (12). The parameters used are the same as in QTCM1 v2.3 and are listed in *SI Appendix, Table S1*. Horizontal derivatives are approximated as differences between values over land and those over ocean, divided by an assumed horizontal length scale of 1,000 km. We changed the sign of v from that used in the original QTCM so that it represents horizontal wind in the lower instead of upper troposphere. The oceanic value of q is assumed to be 5 g·kg⁻¹ moister than the tropical mean profile about which the model's vertical profiles are expanded to first order, and the oceanic value of T is set equal to q so that the oceanic atmosphere is convectively neutral. These choices are consistent with monsoons occurring in regions warmer than the tropical mean, but our results are not qualitatively sensitive to the oceanic values used for T and q . For consistency with Levermann et al. (2), we set E and H to zero and force the circulation through changes in R . This is physically unrealistic, but E , H , and R are all components of Q , and the omission of E and H makes no qualitative difference in our results, consistent with the analysis in Levermann et al. (2).

Our GCM (CESM) is produced by the National Center for Atmospheric Research and has fully coupled and interactive dynamical ocean, atmosphere, land, and sea ice models. These components are integrated at a nominal horizontal resolution of 0.9° × 1.25° with 26 atmospheric vertical levels, using the B_2000 component set with 0.9x1.25_gx1v6 grid. Although CESM has bias relative to observations in its simulation of the South Asian monsoon

(34), it is better than most GCMs in simulating the observed climatology of South Asian rainfall (35). It has been used in multiple studies of the effects of aerosols on the South Asian monsoon (36, 37). One series of integrations was conducted for each type of forcing, all using modern initial and boundary conditions but slightly different CESM versions. For the series in which CO₂ was varied, we used version 1.2.2 with Community Atmosphere Model version 4 (CAM4) physics, run for 100 model years with the last 70 used for analyses. The CO₂ mixing ratio was changed on the first time step of each integration to the given multiple of 367 ppm and fixed thereafter. For the series of runs in which aerosol emissions were varied, we used version 1.2.2 with CAM5 physics, run for 30 y with the last 25 analyzed. We used the aerosol scheme (Modal Aerosol Module version 3) that describes the aerosol size distribution with three log-normal modes (38). Only Asian anthropogenic emissions (from domestic, agricultural, and industrial activity) were changed, with BC and sulfate emissions perturbed separately. For the series in which land surface albedo was changed, we used version 1.0.4 with CAM4 physics, run for 30 y with the last 25 analyzed. In those runs, a time-invariant, horizontally homogeneous, broadband surface shortwave albedo was prescribed over nonelevated parts of India (green contours in Fig. 3B provide rough bounds). Specifically, albedo was modified for land with surface pressure higher than 910 hPa in these three regions: (60°E–90°E, 3°N–27.5°N), (60°E–73°E, 25°N–35°N), and the region 73°E–90°E that lies north of 25°N and south of a line between (73°E, 35°N) and (90°E, 25°N). Code containing the albedo modifications is available from the authors.

The speed of the Somali jet was defined following previous work (9). Composites of the annual cycle of jet speed were produced by averaging over 5 y relative to the onset date, with onset being the start of the first 6-d period, of each calendar year, in which the speed maintained a value more than 1 SD above its climatological annual mean.

ACKNOWLEDGMENTS. W.R.B. thanks Tim Cronin, Ian Eisenman, Nadir Jeevanjee, and Tim Merlis for useful comments. W.R.B. was supported by National Science Foundation Grants AGS-1253222 and AGS-1515960 and Office of Naval Research Grant N000141512531. This work was supported in part by the Yale University Faculty of Arts and Sciences High Performance Computing Center.

- Zickfeld K, Knopf B, Petoukhov V, Schellnhuber H (2005) Is the Indian summer monsoon stable against global change? *Geophys Res Lett* 32(15):L15707.
- Levermann A, Schewe J, Petoukhov V, Held H (2009) Basic mechanism for abrupt monsoon transitions. *Proc Natl Acad Sci USA* 106(49):20572–20577.
- Lenton TM, et al. (2008) Tipping elements in the Earth's climate system. *Proc Natl Acad Sci USA* 105(6):1786–1793.
- Schewe J, Levermann A (2012) A statistically predictive model for future monsoon failure in India. *Environ Res Lett* 7(4):044023.
- Collins M, et al. (2013) *Climate Change 2013: The Physical Science Basis. Contribution of Working Group I to the Fifth Assessment Report of the Intergovernmental Panel on Climate Change*, eds Stocker T, et al. (Cambridge Univ Press, Cambridge, UK).
- Overpeck JT, Cole JE (2006) Abrupt change in Earth's climate system. *Annu Rev Environ Resour* 31:1–31.
- McGee D, et al. (2013) The magnitude, timing and abruptness of changes in North African dust deposition over the last 20,000 yr. *Earth Planet Sci Lett* 371–372:163–176.
- Murakami T, Chen LX, Xie A (1986) Relationship among seasonal cycles, low-frequency oscillations, and transient disturbances as revealed from outgoing longwave radiation data. *Mon Weather Rev* 114(8):1456–1465.
- Boos WR, Emanuel KA (2009) Annual intensification of the Somali jet in a quasi-equilibrium framework: Observational composites. *Q J R Meteorol Soc* 135(639):319–335.
- Bordoni S, Schneider T (2008) Monsoons as eddy-mediated regime transitions of the tropical overturning circulation. *Nat Geosci* 1:515–519.
- Shaw TA (2014) On the role of planetary-scale waves in the abrupt seasonal transition of the Northern Hemisphere general circulation. *J Atmos Sci* 71(5):1724–1746.
- Neelin JD, Zeng N (2000) A quasi-equilibrium tropical circulation model. *Formulation. J Atmos Sci* 57(11):1741–1766.
- Neelin J (2007) *The Global Circulation of the Atmosphere*, eds Schneider T, Sobel AH (Princeton Univ Press, Princeton, NJ), pp 267–301.
- Neelin J, Held I (1987) Modeling tropical convergence based on the moist static energy budget. *Mon Weather Rev* 115(1):3–12.
- Yu J, Chou C, Neelin J (1998) Estimating the gross moist stability of the tropical atmosphere. *J Atmos Sci* 55(8):1354–1372.
- Kuo HL (1965) On formation and intensification of tropical cyclones through latent heat release by cumulus convection. *J Atmos Sci* 22(1):40–63.
- Matsuno T (1966) Quasi-geostrophic motions in the equatorial area. *J Meteorol Soc Jpn* 44(1):25–43.
- Webster PJ (1981) Mechanisms determining the atmospheric response to sea surface temperature anomalies. *J Atmos Sci* 38(3):554–571.
- Sobel A, Bretherton C (2000) Modeling tropical precipitation in a single column. *J Clim* 13(24):4378–4392.
- Trenberth KE, Fasullo JT (2013) Regional energy and water cycles: Transports from ocean to land. *J Clim* 26(20):7837–7851.
- Wang B, Fan Z (1999) Choice of South Asian summer monsoon indices. *Bull Am Meteorol Soc* 80(4):629–638.
- Boos WR, Kuang Z (2013) Sensitivity of the South Asian monsoon to elevated and non-elevated heating. *Sci Rep* 3:1192.
- Ma D, Boos W, Kuang Z (2014) Effects of orography and surface heat fluxes on the south Asian summer monsoon. *J Clim* 27(17):6647–6659.
- Chou C, Wu TC, Tan PH (2013) Changes in gross moist stability in the tropics under global warming. *Clim Dyn* 41(9):2481–2496.
- Ramanathan V, et al. (2005) Atmospheric brown clouds: Impacts on South Asian climate and hydrological cycle. *Proc Natl Acad Sci USA* 102(15):5326–5333.
- Bollasina MA, Ming Y, Ramaswamy V (2011) Anthropogenic aerosols and the weakening of the South Asian summer monsoon. *Science* 334(6055):502–505.
- Chung C, Ramanathan V (2006) Weakening of north Indian SST gradients and the monsoon rainfall in India and the Sahel. *J Clim* 19(10):2036–2045.
- Molnar P, England P, Martinod J (1993) Mantle dynamics, uplift of the Tibetan Plateau, and the Indian monsoon. *Rev Geophys* 31(4):357–396.
- deMenocal P, et al. (2000) Abrupt onset and termination of the African Humid Period: Rapid climate responses to gradual insolation forcing. *Quat Sci Rev* 19:347–361.
- Krishnamurti TN, Ardanuy P, Ramanathan Y, Pasch R (1981) On the onset vortex of the summer monsoon. *Mon Weather Rev* 109(2):344–363.
- Halpern D, Woiceshyn PM (1999) Onset of the Somali jet in the Arabian Sea during June 1997. *J Geophys Res* 104(C8):18041–18046.
- Hales K, Neelin JD, Zeng N (2006) Interaction of vegetation and atmospheric dynamical mechanisms in the mid-Holocene African monsoon. *J Clim* 19(16):4105–4120.
- Neelin JD, Münnich M, Su H, Meyerson JE, Holloway CE (2006) Tropical drying trends in global warming models and observations. *Proc Natl Acad Sci USA* 103(16):6110–6115.
- Boos WR, Hurley JV (2012) Thermodynamic bias in the multimodel mean boreal summer monsoon. *J Clim* 26(7):2279–2287.
- Sperber KR, et al. (2013) The Asian summer monsoon: An intercomparison of CMIP5 vs. CMIP3 simulations of the late 20th century. *Clim Dyn* 41(9):2711–2744.
- Vinoj V, et al. (2014) Short-term modulation of Indian summer monsoon rainfall by West Asian dust. *Nat Geosci* 7(4):308–313.
- Ganguly D, Rasch PJ, Wang H, Yoon JH (2012) Climate response of the South Asian monsoon system to anthropogenic aerosols. *J Geophys Res* 117(D13):D13209.
- Liu X, et al. (2012) Toward a minimal representation of aerosols in climate models: Description and evaluation in the Community Atmosphere Model CAM5. *Geosci Model Dev* 5(3):709–739.

Supporting Information for
“Near-linear response of mean monsoon strength
to a broad range of radiative forcings”

by William R. Boos* & Trude Storelvmo

Department of Geology and Geophysics, Yale University
 PO Box 208109, New Haven, CT, USA

*billboos@alum.mit.edu

Table S1 | Parameters used in our standard analytical model.

Parameter name	symbol	value
Reference gross moisture stratification	M_{qr}	3.0 K
Sensitivity of gross moisture stratification to temperature	M_{qp}	0.05
Reference gross dry stability	M_{sr}	3.6 K
Sensitivity of gross dry stability to temperature	M_{sp}	0.04
Temperature advection coefficient (vertical integral of product of temperature and velocity basis functions)	a_T	-0.31
Moisture advection coefficient (vertical integral of product of humidity and velocity basis functions)	b_T	0.05
Mechanical damping time scale for horizontal wind	$1/\epsilon_1$	3.5 days
Convective response time (rescaled by temperature and humidity basis functions)	τ_c^*	10 hours
Poisson constant (ratio of gas constant to specific heat at constant pressure for dry air)	κ	0.285
Horizontal length scale	L	1000 km

1 Solution of analytical model

We reduce the set (1)-(4) in the main text to a single equation through the following steps. First, all horizontal derivatives are approximated by the difference between land and ocean values over an assumed horizontal length scale L , with v assumed to decay from its maximum value

to zero over this distance in the continental convergence zone. We then rewrite (2) using (1) to replace $\partial T/\partial y$ and using (4) to replace P , yielding

$$\frac{a_T \epsilon_1}{\kappa} V^2 + (M_{sr} + M_{sp} T_L) \frac{V}{L} = \frac{q_L - T_L}{\tau_c^*} \mathcal{H}(q_L - T_L) + R + H \quad (\text{S1})$$

where V is the value of v , the subscripts L and O denote properties over land and ocean, respectively, and the dry stability has been expanded to show its temperature dependence. The discretized moisture equation (3) similarly becomes

$$a_q V \frac{q_L - q_O}{L} - (M_{qr} + M_{qp} q_L) \frac{V}{L} = -\frac{q_L - T_L}{\tau_c^*} \mathcal{H}(q_L - T_L) + E. \quad (\text{S2})$$

We eliminate the Heaviside function by considering the precipitating and non-precipitating regimes separately.

For $P > 0$ (i.e. $q_L > T_L$), we use the discretized moisture equation to solve for q_L ,

$$q_L = \frac{\left(\frac{a_q q_O}{L} + \frac{M_{qr}}{L} + \frac{\epsilon_1 L}{\tau_c^* \kappa}\right) V + E + \frac{T_O}{\tau_c^*}}{\frac{1}{\tau_c^*} + (a_q - M_{qp}) \frac{V}{L}} \quad (\text{S3})$$

where we used (1) to express T_L as

$$T_L = \frac{\epsilon_1 L}{\kappa} V + T_O. \quad (\text{S4})$$

Now we can substitute these expressions for q_L and T_L into the discretized temperature equation (S1), still assuming we are in the $P > 0$ regime, and obtain a single equation in the unknown V ,

$$C_1 V + C_2 V^2 + C_3 V^3 = \frac{E + H + R}{\tau_c^*} \quad (\text{S5})$$

with the constant coefficients

$$\begin{aligned} C_1 &\equiv \frac{1}{L} \left[(H + R) M_{qp} + \frac{1}{\tau_c^*} (M_{sr} - M_{qr} + T_O (M_{sp} - M_{qp})) - a_q \left(H + \frac{q_O - T_O}{\tau_c^*} + R \right) \right] \\ C_2 &\equiv (a_T + a_q + M_{sp} - M_{qp}) \frac{\epsilon_1}{\kappa \tau_c^*} + \frac{a_q - M_{qp}}{L^2} (M_{sr} + M_{sp} T_O) \\ C_3 &\equiv \frac{\epsilon_1}{\kappa L} (a_q - M_{qp}) (a_T + M_{sp}). \end{aligned} \quad (\text{S6})$$

For $P = 0$ (i.e. $q_L \leq T_L$), the equation is much simpler:

$$\frac{1}{L} (M_{sr} + M_{sp} T_O) V + \frac{\epsilon_1}{\kappa} (a_T + M_{sp}) V^2 = H + R. \quad (\text{S7})$$

As described in the Methods section, (S5) and (S7) are solved as a function of Q , assuming that $Q = R$ for consistency with Levermann et al. (2009), and using the the parameter values in Table S1. Relaxing this to allow E and H to be nonzero does not qualitatively change the results.

2 Comparison of analytical model with previous “tipping point” models

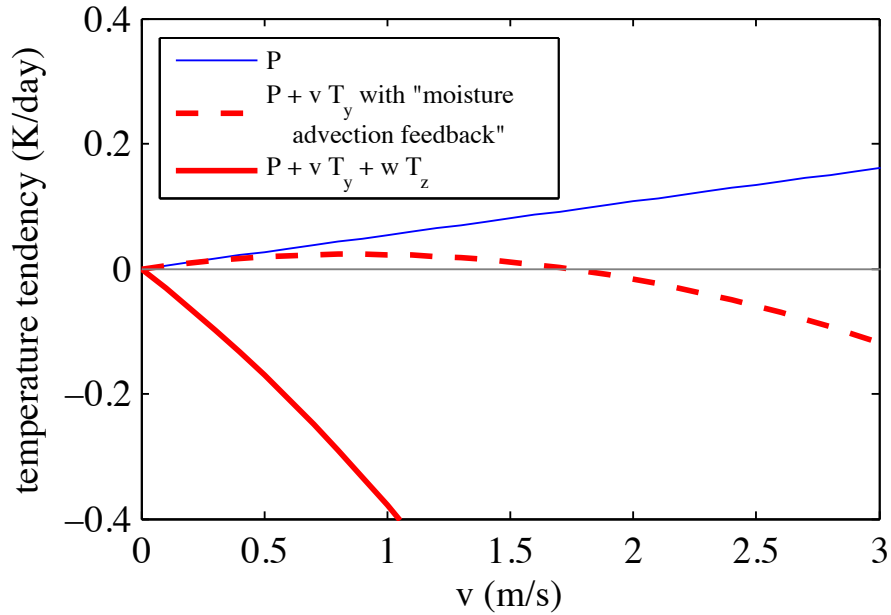
The analytical model consisting of (1)-(4) in the main text can be modified to be isomorphic to that used in Levermann et al. (2009, hereafter L09)¹, who found the monsoon abruptly ceases to exist once the net atmospheric energy source Q becomes more negative than a critical value.

The key change needed to obtain a threshold response is setting $M_s = 0$ K, which sets the dry static stability of the troposphere to zero. But if M_s is set to zero, it is also necessary to change the sign of a_T so that horizontal temperature advection takes the sign of the advection accomplished by the low-level wind. In our standard model and in the full version of the QTCM², vertically integrated horizontal temperature advection is dominated by upper-tropospheric winds because a horizontal temperature gradient has its largest magnitude in the upper troposphere in a moist adiabatic atmosphere (recall that all of our conservation equations describe a first-baroclinic mode that is defined throughout the depth of the troposphere). If the adiabatic cooling that occurs in ascending regions is removed from the model by setting $M_s = 0$ K and if $Q > 0$, horizontal advection is the only remaining temperature tendency that could balance the net diabatic sum of precipitation and radiative flux convergence. Changing the sign of a_T makes its sign consistent with that used in L09. This is overall a minor issue since our standard model yields qualitatively similar results regardless of the sign of a_T , confirming that setting M_s to zero is the primary cause of the spurious bifurcation. When M_s is set to zero and the sign of a_T is changed from its standard value of -0.31 to +0.31, the dashed curve in Fig. 1a is obtained as the solution for P . The solution for v resembles that obtained for P and, as expected, has a bifurcation at the same value of Q .

Further changes are necessary to make (1)-(4) exactly isomorphic to the equations used in L09. The moisture stratification M_q must also be set to 0 K, which eliminates the horizontal convergence of moisture. This is why L09 argued for the existence of a moisture *advection* feedback rather than a moisture *convergence* feedback. It is also necessary to neglect T in (4), which is equivalent to assuming that the latent heating of precipitating convection does not stabilize the column to further convection. When all of these changes are made, a solution for P that is qualitatively similar to that shown by the dashed line in Fig. 1a is obtained. The sum of the temperature tendencies due to precipitation and horizontal temperature advection is then positive and maximum for a monsoon circulation of intermediate strength (dashed line in Fig. S1), as discussed by L09. If the temperature tendency due to adiabatic cooling in ascending regions is added to this sum (by setting M_s to its value in Table S1), the total is instead negative for all values of landward flow (solid red line in Fig. S1), consistent with the fact that adiabatic cooling due to ascent is typically large compared to horizontal temperature advection.

Precipitation renders atmospheric dynamics inherently nonlinear³ because rainfall cannot be negative, and we do not intend to imply that it is impossible for precipitating large-scale circulations to respond nonlinearly to a forcing. Even horizontal shifts in the strong spatial

gradients of moisture that exist at the edges of strongly precipitating regions cannot be dismissed as a simple linear response; theories of convective margins predict such horizontal shifts in terms of how far the moisture content of low-level inflow is from a threshold needed to maintain deep convection.⁴ However, those thresholds seem most relevant on daily time scales, with internal atmospheric variability smoothing the edges of convective zones on monthly and longer periods.⁵



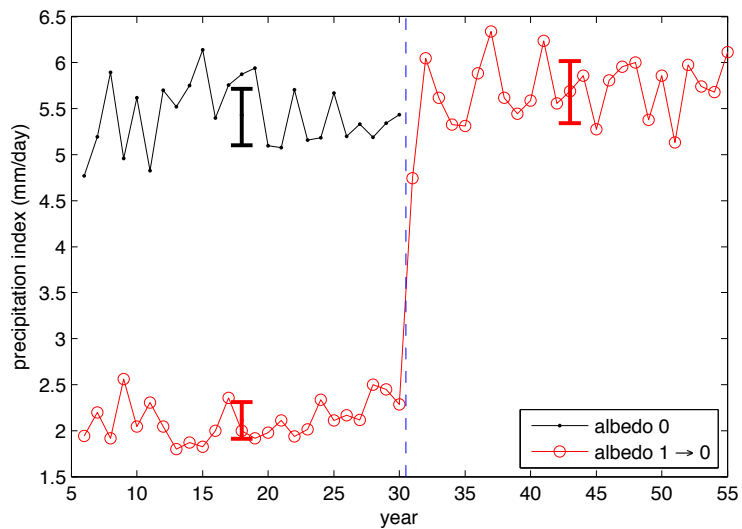
Supplementary Figure S1 | Temperature tendencies over land as a function of circulation strength when our analytical model is made isomorphic to that of L09, as described above. Thin blue line shows the tendency due to latent heating by precipitation, dashed line shows the sum of latent heating and horizontal temperature advection, and solid red line shows the total when the model is augmented with a positive static stability (the total being the sum of latent heating, horizontal temperature advection, and adiabatic cooling due to ascent).

Table S2 | Summary of global climate model integrations. Each row describes a series of integrations, with the left column stating the quantity that was varied, the middle column the factors by which that forcing was multiplied, and the right column the duration of each integration. In the last row the “forcing multiplier” is simply the imposed horizontally uniform land surface albedo. See Methods section for more details.

Forcing type	Forcing multiplier	Duration
CO ₂ amount	0.25, 0.5, 1, 2, 4, 8, 16	100 years
Asian black carbon aerosol emissions	0.25, 0.5, 1, 2, 4, 8, 16	30 years
Asian sulfate aerosol emissions	0.25, 0.5, 1, 2, 4, 8, 16	30 years
India surface albedo	0.0, 0.2, 0.4, 0.6, 0.8, 1.0	30 years

3 Lack of evidence for hysteresis

Although the phrase “tipping point” is often used quite loosely to refer to multiple different properties of a variety of systems, the phrase itself connotes the existence of hysteresis in a system. Studies of tipping points in monsoons used the term only to refer to the discontinuous transition between two stable states as a forcing is increased past a threshold, and did not argue for any hysteresis in monsoons.¹ Nevertheless, we performed a GCM simulation to test whether hysteresis exists. In particular, after integrating our GCM for 30 years with the surface albedo of India set to unity, we changed the albedo of India to zero instantaneously at the start of year 31. By the second year after this change, the strength of the South Asian summer monsoon had reached the same time-mean value as in the 30-year integration that was started at an albedo of zero (Fig. S2). A similar result was obtained when the albedo was changed at the start of year 31 to the default distribution used in the GCM. Thus, there is no evidence for hysteresis when land surface albedo is used as the forcing.



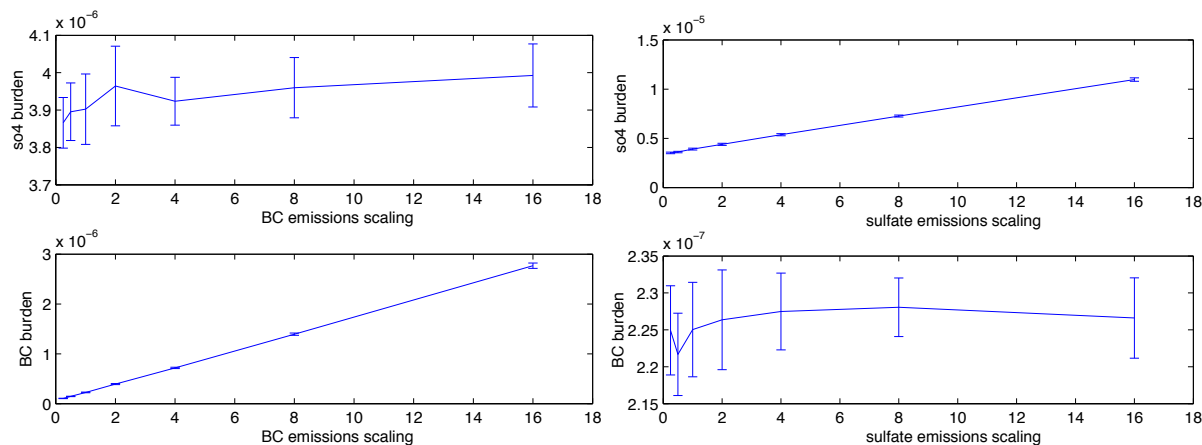
Supplementary Figure S2 | Time series of the South Asian monsoon precipitation index (described in Fig. 2) for the integration with India's surface albedo set to zero (black) and for the integration in which India's surface albedo was started at unity and reduced to zero at the start of year 31 (red). One point is plotted for each summer mean (May-Sept.) value of the precipitation index. Black vertical bar shows the 95% confidence interval for the mean, estimated by 2000 iterations of a bootstrap, for the zero albedo integration, and the two red bars show the same confidence interval for the periods before and after the albedo is changed in the other integration.

4 Additional details on the response to aerosol forcings

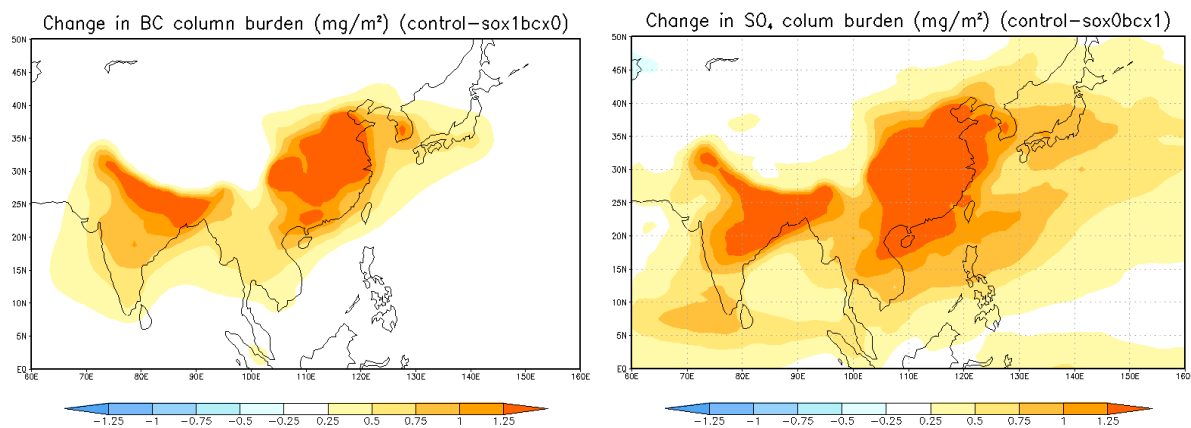
Several previous studies argued that anthropogenic aerosols have reduced South Asian monsoon rainfall in the observational record.^{6,7} Our aerosol perturbations are idealized and not directly comparable to those applied in those previous studies because (i) we perturb only Asian, as opposed to global, aerosol emissions, and (ii) we perturb BC and sulfate separately as opposed to simultaneously as in most studies. Nevertheless, a qualitative comparison with previous work can still be made. For example, Ramanathan et al. (2005) found that the “Asian Brown Cloud” of mixed aerosols reduced the surface shortwave radiative flux over South Asia (0°-30°N and 60°-100°E) by 10-15 W m⁻² between 1930 and the present. In comparison, here the highest sulfur and BC emissions (16×) reduce surface shortwave by 8 and 10 W m⁻², respectively, relative to the control (1×). Relative to the control simulation, the simulations with the highest sulfur and BC emissions show a reduction in rainfall over South Asia of about 10% and 5%, respectively. For comparison, Ramanathan et al. (2005) found a rainfall reduction of 8-10% in the same region in response to the Asian Brown Cloud. For the much smaller region of Northern India (20°-28°N and 60°-100°E), Bollasina et al. (2008) found a precipitation reduction due to all anthropogenic aerosols of about 0.4 mm day⁻¹, whereas a reduction of around 0.2 mm day⁻¹ is obtained for our highest aerosol emissions. Consistent with Bollasina et al. (2008), the rainfall reduction in this region is mainly caused by the increase in sulfate aerosols.

Although anthropogenic emissions vary by a factor of 64 over our entire range of forcings, the column burden of sulfate and black carbon averaged over the same time and space domain used for our precipitation index vary only by 2.5 and 30, respectively. Aerosol burden scales linearly with emissions (Fig. S3). The weaker response of the sulfate burden to changes in anthropogenic emissions is expected due to its more abundant natural sources, as well as significant sulfate transport from surrounding source regions. Although there are surely biases in the treatment of aerosols in CESM, this illustrates the degree to which deposition and transport reduce aerosol concentrations, especially during the summer monsoon season when wet deposition by precipitation is highly active. It also illustrates the potential problem with using prescribed aerosol concentrations or radiative forcings that cannot be influenced by winds or precipitation.

Finally, Fig. S4 shows the spatial distribution of sulfate and BC aerosol burdens attributable to anthropogenic emissions in the control simulation. These emissions are multiplied by the factors in Table S2 in order to simulate perturbations to Asian emissions of aerosols and their precursors.



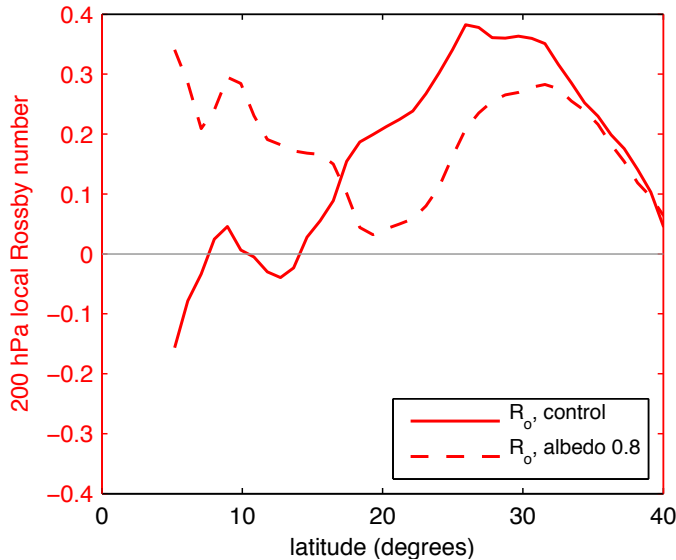
Supplementary Figure S3 | Time- and spatial-mean burdens of sulfate aerosol (top panels) and BC aerosol (bottom panels), in kg m^{-2} , as a function of the factor by which Asian anthropogenic emissions are scaled. Left panels show the response to variations in BC emissions, while right panels show response to variations in sulfate emissions. Time averages are taken from May-September over 25 model years, and spatial averages from $50\text{-}110^\circ\text{E}$, $10\text{-}35^\circ\text{N}$.



Supplementary Figure S4 | Atmospheric column burdens (mg m^{-2}) of BC aerosol (left) and sulfate aerosol (right) attributable to anthropogenic emissions, calculated as the difference in burdens between the control simulation and simulations in which anthropogenic emissions of BC and sulfate (including precursors) were set to zero, respectively.

5 Response of dynamical nonlinearities to large albedo forcings

The main text showed that the ascent branch of the circulation shifts toward the equator in response to a large increase in land surface albedo. Here we show that the region of nonlinear upper tropospheric dynamics also shifts toward the equator in response to that forcing. We define the local Rossby number R_o as $-\bar{\zeta}/f$, where ζ is the vertical component of relative vorticity, f the Coriolis parameter, and an overbar denotes a time mean over the 20 days following monsoon onset. R_o is zero in linear dynamical regimes and approaches unity in the nonlinear limit of zero absolute vorticity.⁸ When the surface albedo is increased from its control value to 0.8 over India, there is an increase in upper-tropospheric R_o south of India and a decrease of R_o over South Asia. Increased albedo thus shifts the dynamically nonlinear region toward the equator. Thus, nonlinear atmospheric dynamics still occur for even the strongest albedo forcings, but shift toward the equator together with the ascent branch of the circulation.



Supplementary Figure S5 | Upper-tropospheric local Rossby number in the GCM integration with default albedo (solid lines) and with the land surface albedo of continental India set to 0.8 (dashed lines). Rossby number is averaged 50-90°E and over 5 years during the 20-day period after which jet onset occurs within each year.

References

1. Levermann, A., Schewe, J., Petoukhov, V. & Held, H. Basic mechanism for abrupt monsoon transitions. *Proc. Natl. Acad. Sci. USA* **106**, 20572–20577 (2009).
2. Neelin, J. D. & Zeng, N. A quasi-equilibrium tropical circulation model: Formulation. *J. Atmos. Sci.* **57**, 1741–1766 (2000).
3. Frierson, D., Majda, A. & Pauluis, O. Large-scale dynamics of precipitation fronts in the tropical atmosphere: a novel relaxation limit. *Commun. Math. Sci* **2**, 591–626 (2004).
4. Lintner, B. R. & Neelin, J. D. Soil Moisture Impacts on Convective Margins. *Journal of Hydrometeorology* **10**, 1026–1039 (2009).
5. Lintner, B. R. & Neelin, J. D. A prototype for convective margin shifts. *Geophysical Research Letters* **34**, 1–5 (2007).
6. Ramanathan, V. *et al.* Atmospheric brown clouds: Impacts on South Asian climate and hydrological cycle. *Proc. Natl. Acad. Sci. USA* **102**, 5326 (2005).
7. Bollasina, M. A., Ming, Y. & Ramaswamy, V. Anthropogenic aerosols and the weakening of the South Asian summer monsoon. *Science* **334**, 502–505 (2011).
8. Walker, C. C. & Schneider, T. Eddy influences on Hadley circulations: simulations with an idealized GCM. *J. Atmos. Sci.* **63**, 3333–3350 (2006).